Computational and Structural Biotechnology Journal 21 (2023) 3196–3209

Contents lists available at ScienceDirect

Computational and Structural Biotechnology Journal

journal homepage: www.elsevier.com/locate/csbj

Research article

Unique features of the TCR repertoire of reactivated memory T cells in the experimental mouse tumor model

Anastasiia Kalinina [a], Nadezda Persiyantseva [a], Olga Britanova [b,c], Ksenia Lupyr [d,e], Irina Shagina [b,c], Ludmila Khromykh [a], Dmitry Kazansky [a,*]

[a] N.N. Blokhin National Medical Research Center of Oncology of the Ministry of Health of the Russian Federation, Kashirskoe sh. 24, 115478 Moscow, Russian Federation
[b] Shemyakin-Ovchinnikov Institute of Bioorganic Chemistry, Russian Academy of Sciences, Miklukho-Maklaya st. 16/10, 117997 Moscow, Russian Federation
[c] Institute of Translational Medicine, Pirogov Russian National Research Medical University, Ostrovityanova st.1, 17997 Moscow, Russian Federation
[d] Center of Life Sciences, Skolkovo Institute of Science and Technology, Bolshoi boulevard 30c1, 121205 Moscow, Russian Federation
[e] Institute of Translational Medicine, Center for Precision Genome Editing and Genetic Technologies for Biomedicine, Pirogov Russian National Research Medical University, Ostrovityanova st.1,build. 1, 17997 Moscow, Russian Federation

ARTICLE INFO

Article history:
Received 10 March 2023
Received in revised form 24 May 2023
Accepted 24 May 2023
Available online 26 May 2023

Keywords:
T cell receptor
TCR repertoire
TCR physicochemical features
Memory cells
Antigen-specific clonotypes
NGS sequencing
Bioinformatics
Adoptive cell therapy
TCR chain centricity

ABSTRACT

T cell engineering with T cell receptors (TCR) specific to tumor antigens has become a breakthrough towards personalized cancer adoptive cell immunotherapy. However, the search for therapeutic TCRs is often challenging, and effective strategies are strongly required for the identification and enrichment of tumor-specific T cells that express TCRs with superior functional characteristics. Using an experimental mouse tumor model, we studied sequential changes in TCR repertoire features of T cells involved in the primary and secondary immune responses to allogeneic tumor antigens. In-depth bioinformatics analysis of TCR repertoires showed differences in reactivated memory T cells compared to primarily activated effectors. After cognate antigen re-encounter, memory cells were enriched with clonotypes that express α-chain TCR with high potential cross-reactivity and enhanced strength of interaction with both MHC and docked peptides. Our findings suggest that functionally true memory T cells could be a better source of therapeutic TCRs for adoptive cell therapy. No marked changes were observed in the physicochemical characteristics of TCRβ in reactivated memory clonotypes, indicative of the dominant role of TCRα in the secondary allogeneic immune response. The results of this study could further contribute to the development of TCR-modified T cell products based on the phenomenon of TCR chain centricity.

1. Introduction

T lymphocytes are crucial players in adaptive anti-tumor immunity. To accomplish their functions, T cells are equipped with a highly specialized receptor, the T cell receptor (TCR), which recognizes short peptide antigens bound to self-major histocompatibility complexes (pMHC complexes). In the predominant T cell subset, TCR is a heterodimer composed of an α- and β-chain. TCR shaping begins in an immature thymocyte with the β-chain rearrangement from one allele, starting with the rearrangement of the D and J gene segments and followed by the junction of the V segment. After the development of a productive in-frame TCRβ, the TCRα rearrangement begins and involves V and J recombination [1]. Both α- and β-chain TCR contain three complementarity-determining regions (CDRs), which mainly contribute to pMHC recognition. The CDR1 and CDR2 regions primarily make contacts with an MHC molecule, while CDR3 mediates TCR interaction with a docked antigen [2]. Therefore, CDR3α and CDR3β are the structural basis of the clonal specificity of T lymphocytes.

Gene modification of T cells with TCRs or chimeric antigen receptors (CAR) has become a powerful tool for cancer immunotherapy

Abbreviation: TCR -, T cell receptor; TCRα/β -, α/β-chain of a T cell receptor; MHC -, major histocompatibility complex; pMHC -, peptide-MHC complex; CDR -, complementarity-determining region; CAR-, chimeric antigen receptor; TAA-, tumor-associated antigen; ACT-, adoptive cell therapy; MitC-, mitomycin C; HS-, heat shock; UMI-, unique molecular identifier; AA-, amino acid; Pgen-, probability of clonotype generation

* Correspondence to: Federal State Budgetary Institution "N.N. Blokhin National Medical Research Center of Oncology" of the Ministry of Health of the Russian Federation, Kashirskoe sh., 24, Moscow 115478, Russian Federation.
E-mail address: kazansky1@yandex.ru (D. Kazansky).

https://doi.org/10.1016/j.csbj.2023.05.028

[3,4]. CAR-T cells are independent of pMHC-TCR interactions and, therefore, recognize a specific antigen in a non-MHC-restricted manner. However, CAR-T cells are unable to eliminate malignant cells bearing intracellular neoantigens and mainly target tumor-associated antigens (TAA). This limits the applicability of CAR-T cell therapy. TCR-engineered T cells can target both TAA and tumor-specific antigens in complex with a patient's MHC. In this respect, TCR-T cell therapy is more versatile and can be applied to more cancers, but it is always personalized due to MHC polymorphisms.

The search for therapeutic TCRs is rather tricky, largely depending on the selection of target tumor antigens. Tumor neoantigens are the best targets for adoptive T cell therapy (ACT) [4,5]. However, such antigens are often subjected to immunoediting under the pressure of the host immune response, resulting in the selection of less immunogenic malignant cell clones and contributing to tumor progression [5]. TAA and cancer germline antigens are alternative targets, but they are essentially self-antigens that are expressed at low levels in normal (non-tumor) tissues [5]. As such, only low-affinity TCRs can be found for such antigens due to the elimination of highly autoreactive T cells by mechanisms of central and peripheral tolerance [2,5,6]. Considering that high TCR-pMHC binding affinity/avidity is required to reach the clinical benefit of TCR-T cell ACT [7,8], many efforts are put into improving TCR affinity to chosen tumor antigens [2,7]. However, TCRs with artificially enhanced affinity/avidity impose risks of off-tumor on-target and off-target toxicities [3,4,7].

In this light, the application of memory T cells in ACT could be a promising strategy [9]. The repertoire of memory T cells was shown to be enriched in clonotypes with high affinity/avidity TCRs as the result of antigen-driven clonal expansion [7,10]. Furthermore, compared to effectors and effector memory T cells, long-lived central memory T cells display more potent anti-tumor activity, better proliferate, and persist longer in vivo after transfusion to a patient [9,11,12]. Central memory T cells were proposed as a better subset to be used for the generation of T cell products for ACT [12], but they can also be viewed as the best source of therapeutic TCRs with superior functional characteristics.

Approaches for identifying and expanding tumor antigen-specific T lymphocytes are now being actively developed, and bioinformatics has become a valuable tool to detect clonotypes involved in immune responses [13–16]. Still, efficient bioinformatics strategies are required to identify distinct functional T cell subsets in bulk repertoires with a view to finding antigen-specific clonotypes with the required functional features. A recent study discovered that TCR repertoires of different functional subsets of human effector/memory T cells exhibited specific physicochemical properties [17]. In the study here, we aimed to further characterize TCR features of antigen-specific memory T cells and follow sequential changes in TCR repertoires of T cells involved in the primary and secondary immune responses. For this, we exploited an experimental mouse model of induction of the immune response to the allogeneic tumor [18]. We defined prominent TCR characteristics in reactivated memory T cells that differed from those of primarily activated effectors. In our experimental system, in the secondary immune response, memory T cells relied on TCRα, which strongly interacted with both MHC and docked peptides. The findings of this study could contribute to the development of efficient techniques for identifying and enriching functionally true memory T cells, which could be a better source of therapeutic TCRs for ACT.

2. Materials and methods

2.1. Study design

To track changes in TCR repertoires during the primary and secondary immune responses, we exploited an experimental mouse model of induction of the immune response in C57BL/6 mice (of the H2-K^b haplotype) to mastocytoma P815 (K^dD^d) [18]. Due to differences in MHC class I molecules, P815 tumor cells elicit a strong $CD8^+$ allogeneic response in these mice. As previously described [18], long-lived central memory cells are established in immunized C57BL/6 mice two months following in vivo P815 cell transplantation. Our recent study showed that the phenotypic characteristics of T cells (especially the expression of the CD44 molecule in mice) didn't necessarily correlate with their actual antigenic experience [19]. Accordingly, identification of true memory cells based exclusively on the surface phenotype is not always correct, and validation of their functional properties is required [19]. Taking this into account, in the studies here, we relied mainly on the previously developed functional test [18,20], which allows for selective activation of antigen-specific memory T cells by in vitro re-challenge with cognate stimulator cells exposed to acute heat shock (HS). It was shown that HS inhibits the expression of the co-stimulatory molecule B7–1 (CD80) on antigen-presenting cells [20]. Furthermore, cells exposed to HS cannot rearrange their cytoskeleton and, hence, form a stable immunological synapse with a T cell [21,22]. Thus, HS-exposed cells provide insufficient co-stimulation to T cells and cannot activate naive T cells that are strongly dependent on proper co-stimulation stimuli. In contrast, memory T cells were shown to be relatively independent of co-stimulation signals [20,23], and they can respond to HS-treated cognate stimulators after receiving the antigen-specific signal from them via TCRs [18,20]. Therefore, the developed functional test [18,20] is a reliable and reproducible method to selectively and specifically reactivate memory T cells in vitro. Compared to HS, treatment with cytostatic mitomycin C (MitC) only blocks stimulator cell proliferation without affecting their co-stimulatory capacity. Hence, both naive (antigen-inexperienced) and memory T cells could respond to MitC-treated stimulators. To induce the primary immune response, lymphocytes from non-immunized C57BL/6 mice were co-cultured in vitro with MitC-treated P815 cells. This provoked the proliferation of predominantly $CD8^+$ T cells in response to allogeneic tumor antigens (Supplementary Fig. 1) [18]. Features of the TCRα/β repertoires of these primarily activated effector T cells were compared with the initial repertoires of T lymphocytes in the same intact mouse without antigenic stimulation. To study TCR repertoire reshaping during the secondary immune response, lymphocytes of the P815-immunized mouse were reactivated in vitro by the cognate allogeneic stimulators (P815 cells) treated with MitC (Supplementary Fig. 1). Lymphocytes from the same immunized mouse were co-cultured with mastocytoma cells exposed to HS to selectively reactivate long-lived central memory cells formed by in vivo immunization with P815 (Supplementary Fig. 1) [18,20]. The repertoires of TCRα and TCRβ memory clonotypes formed under both stimulating conditions were compared to the TCRα/β repertoires of the same P815-immunized mouse without re-stimulation. Accordingly, we were able to evaluate the sequential reshaping of the TCR repertoire in the course of the allogeneic immune response in mice, starting from the primary response to the formation of immunological memory and the induction of the secondary immune response of memory cells.

2.2. Animals

Female C57BL/6 ($K^bI\text{-}A^bD^b$) mice (18–22 g, 6–8-wk-of-age) were obtained from the breeding facility of N.N. Blokhin National Medical Research Center of Oncology of the Ministry of Health of the Russian Federation (N.N. Blokhin NMRCO, Moscow, Russia). Nonetheless, male mice can also be used in the studies described here, as sex differences are insignificant and do not introduce variability to the outcomes of the developed experimental system. Mice were housed in facilities maintained at 20–24ºC with a 40% relative humidity and a 12-hour light/dark cycle. All mice had ad libitum access to standard rodent chow and filtered tap water. Mice were handled in strict

compliance with the NIH guide for the care and use of laboratory animals (8th edition, 2011). All the experimental procedures were approved by the Ethics Committee on Animal Experimentation of N.N. Blokhin NMRCO.

2.3. Tumor cell line, immunization of mice

Murine mastocytoma P815 (K^dD^d) (TIB-64, ATCC) was cultured in RPMI-1640 medium (PanEco, Moscow, Russia) supplemented with 10% fetal bovine serum (HyClone, GE Healthcare, Chicago, IL), 0.01 mg/ml ciprofloxacin (KRKA, Novo Mesto, Slovenia), and 0.01 M HEPES (PanEco) (complete RPMI). Tumor cells at 70% confluence were harvested, washed three times in phosphate-buffered saline (PBS) by centrifugation (200 x g, 5 min, 4 °C), and counted in a hemocytometer after trypan blue/eosin (mixed 1:1 *v/v*) staining. C57BL/6 mice were immunized intraperitoneally with 1×10^7 P815 cells in 500 μl of PBS. Two months later, P815-immunized mice with developed long-lived memory T cells (MEMO mice) were sacrificed by cervical dislocation; their spleens were aseptically isolated and gently homogenized in a Potter homogenizer in 3 ml of sterile PBS. Cell suspensions were centrifuged, resuspended in 3 ml of complete RPMI, and counted as described above. Splenocyte suspensions from non-immunized (intact) C57BL/6 mice were similarly prepared and used for comparison in these studies.

2.4. Mixed lymphocyte-tumor culture

Spleen cells (4.0×10^5) from P815-immunized (MEMO) and non-immunized (intact) C57BL/6 mice were seeded in triplets in 96-well flat-bottom plates (Corning Costar, Sigma Aldrich, St. Louis, MO) in 100 μl of complete RPMI supplemented with 10 mM 2-mercaptoethanol (Merck, Darmstadt, Germany) (the supplemented complete medium). P815 cells at 70% confluence were harvested, treated with MitC (Kyowa Hakko Kogyo Co., Ltd., Japan) (50 μg/ml, 37 °C, 1 h), and washed three times in PBS by centrifugation (200 x g, 5 min, 4 °C). Alternatively, P815 cells were exposed to HS at 45 °C for 1 h. MitC- and HS-treated tumor cells were used as stimulators for spleen cells from MEMO and intact mice. For this, 4.0×10^4 MitC- or HS-treated P815 cells were added to splenocytes from intact and MEMO mice in 100 μl of the supplemented complete medium to a final volume of 200 μl. Cells were cultured at 37 °C with 5% CO2 for 72 h. Splenocytes similarly cultured alone were used to evaluate the background cell proliferation. Cell proliferation was measured by the incorporation of ^{3}H-thymidine (Isotop, Moscow, Russia) added in the last 16–18 h of culturing using a liquid scintillation β-counter (LKB, Stockholm, Sweden). The level of cell proliferative activity was expressed as the number of counts per minute (cpm). To calculate the antigen-induced immune response, the respective level of the background proliferation was subtracted from the level of cell proliferation in the presence of stimulators (P815_MitC or P815_HS).

2.5. Generation of cDNA libraries

Cell suspensions were prepared as described above from spleens harvested individually from one non-immunized (intact) and one P815-immunized (MEMO) C57BL/6 mouse. The splenocytes were cultured in vitro with P815 tumor cells (MitC-treated for an intact mouse and both MitC- and HS-treated for the MEMO mouse) as described in the previous section. In parallel, the splenocytes of these two mice were similarly cultured without antigenic stimulation. After 72 h of in vitro culture, $1.0–1.5 \times 10^6$ spleen cells of each mouse in each culture condition were used for RNA isolation using the TRI reagent (MRC, Inc., Cincinnati, OH). Using all amounts of isolated RNA, cDNA libraries of TCRα and TCRβ of each mouse were prepared as described earlier [24]. After two rounds of PCR amplification as described by Egorov et al. [24], the samples were purified and true-seq adapters were ligated according to the manufacturer's recommendations (Illumina, San Diego, CA). Next-generation sequencing was performed on the MiSeq platform (Illumina) using the Myseq reagent kit (300 cycles). Raw data was processed using MiGEC [25]. The data was processed with a threshold of six reads per unique molecular identifier (UMI) for all samples. CDR3-containing reads labeled with identical UMIs were assembled into a single molecular identifier group. Further clonotype extraction from the MiGEC-assembled data was performed using MiXCR software [26]. The algorithm for the bioinformatics data analysis is presented in Supplementary Figure 2. As a result, four cDNA libraries were generated for one non-immunized (intact) mouse: two for TCRα clonotypes and two for TCRβ clonotypes with or without in vitro stimulation with MitC-treated mastocytoma P815 (Intact without St and Intact+P815_MitC, respectively). Six cDNA libraries were generated for one P815-immunized (MEMO) mouse: three for TCRα clonotypes and three for TCRβ clonotypes. The TCRa/β MEMO libraries included one without in vitro stimulation (MEMO without St), one with MitC-treated P815 stimulation (MEMO+P815_MitC), and one with heat shock-treated P815 stimulation (MEMO +P815_HS).

2.6. Bioinformatics analysis of the generated TCRα and TCRβ repertoires

The total count of identified UMIs and the total clonotype diversity in each generated TCRα and TCRβ repertoire are presented in Table 1. To evaluate the uniformity of clonotype sizes, the Shannon-Wiener diversity index was calculated for each repertoire. The Chao1 index was also calculated in each repertoire to assess the diversity based on the abundance of clonotypes. As diversity, the Shannon-Wiener and Chao1 indices strongly depend on the total counts of identified clonotypes, which are different in each experimental group (Table 1), all repertoires were normalized by the minimal UMI count of 33699 (Table 1). Normalized indices were calculated for each TCRα and TCRβ repertoire.

2.7. Search for overrepresented clusters of homologous TCRs

The distance between TCRs was calculated using the trcdist metrics [15] by the tcrdist3 package [27]. For each clonotype, neighbors with a distance of less than 16 were discovered. The Fisher exact test was then used to determine the association between the sum of counts of homologous clonotypes and the group for each clonotype. The probability of CDR3 sequence generation (Pgen) was also calculated as described elsewhere [27] for TCRα and TCRβ clonotypes in the repertoire of intact and MEMO mice after in vitro antigenic stimulation (i.e., for expanded clonotypes of primarily activated effectors and reactivated memory T cells, respectively).

2.8. Analysis of physicochemical properties of TCRα and TCRβ CDR regions

The physicochemical properties of amino acids (AA) in V-germ and the CDR3 region were analyzed for the TOP-100 most frequent clonotypes in each generated TCRα and TCRβ repertoire. Evaluations were performed using VDJtools [28] (Supplementary Fig. 2). The mean values of strength (an estimated value of interaction affinities between AA pairs at the CDR3-peptide interface), hydropathy, charge, volume, and polarity were calculated for the full CDR3 region of the TOP-100 TCRα and TCRβ clonotypes in each generated repertoire. AA diversity and distribution, as well as the utilization of strongly interacting and hydrophobic AA, were also analyzed for the five central residues of CDR3 (cCDR3) of the TOP-100 TCRα and TCRβ clonotypes in each repertoire. The Shannon entropy of cCDR3α/β was calculated as described elsewhere [29].

Table 1
The total and normalized TCRα (A) and TCRβ (B) repertoire diversity in the individual non-immunized (intact) and P815-immunized (MEMO) C57BL/6 mouse with or without in vitro stimulation with mastocytoma P815.

A)Group	TCRα				
	Total UMI count	Total diversity	Normalized diversity	Normalized Shannon-Wiener diversity index	Normalized Chao1 index
Intact without St	44805	20476	16515	0.92	54470
Intact+P815_MitC	48128	18751	14545	0.92	46010
MEMO without St	33699	13650	13650	0.90	38840
MEMO+P815_MitC	120980	10129	6262	0.90	9454
MEMO+P815_HS	112265	10196	6151	0.90	10063
B)Group	**TCRβ**				
	Total UMI count	**Total diversity**	**Normalized diversity**	**Normalized Shannon-Wiener diversity index**	**Normalized Chao1 index**
Intact without St	64114	32626	19611	0.92	78671
Intact+P815_MitC	66063	24780	14809	0.91	60964
MEMO without St	52564	23257	16714	0.92	54580
MEMO+P815_MitC	150677	12341	6735	0.90	10813
MEMO+P815_HS	164669	14473	6897	0.90	12034

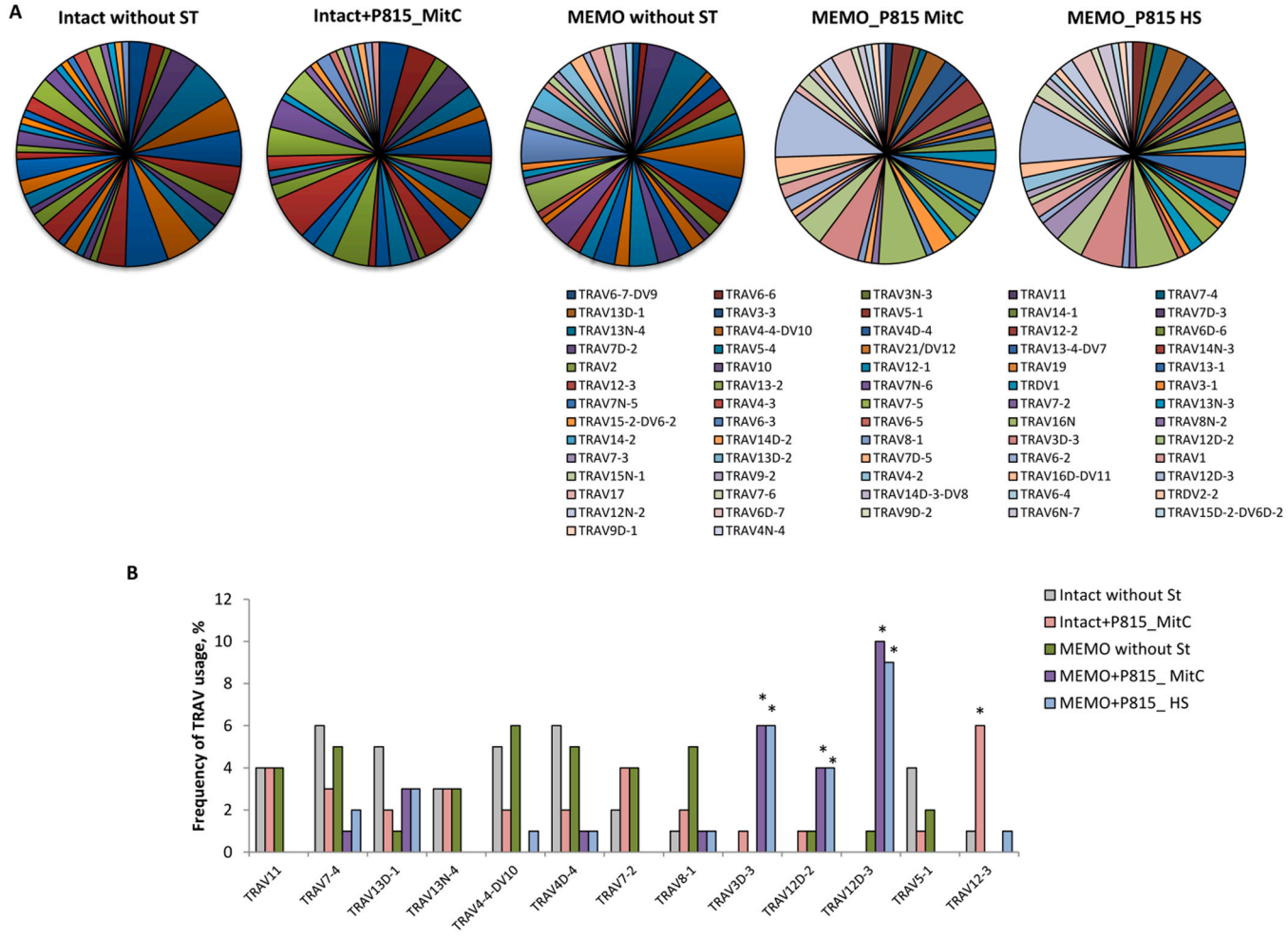

Fig. 1. Utilization of TRAV gene segments in the TOP-100 clonotypes of intact and P815-immunized mice after in vitro stimulation with P815. Splenocytes of the non-immunized (intact) or P815-immunized (MEMO) C57BL/6 mouse were cultured in vitro for 72 h without stimulation (without St) or with mastocytoma P815 cells treated with mitomycin C (P815_MitC) or acute heat shock (P815_HS). Following that, TCRα and TCRβ repertoires were generated for each culture group. A) The use of TRAV gene segments (%) in the TOP-100 largest clonotypes in the repertoires of the intact and MEMO mice with and without in vitro stimulation. B) The discrepant use of individual TRAV gene segments (%) in the TOP-100 largest clonotypes in the repertoires of the intact and MEMO mice after in vitro stimulation. * $p < 0.05$ (Mann-Whitney U-test for comparison Intact+P815_MitC vs. Intact without St; Kruskal-Wallis test and Dunn's test for comparisons: MEMO+P815_MitC vs. MEMO without St and MEMO+P815_HS vs. MEMO without St).

2.9. Statistical analysis

Data are presented as mean ± SEM. The data sets of CDR physicochemical properties didn't fit the normal distribution as analyzed by the Shapiro-Wilk test. Statistical analyses were performed using the unpaired Student's t-test, the Mann-Whitney U-test, and the Wilcoxon signed-rank test. For intragroup comparison of the repertoires of the MEMO mouse, the Wilcoxon signed-rank test (two-tailed), the Kruskal-Wallis test, and the Dunn's test were used. A p-value < 0.05 was considered significant. All statistical analyses were performed using Statistica for Windows 6.0 (StatSoft Inc., Tulsa, OK) and Prism software (v. 8.1.2, GraphPad, San Diego, CA).

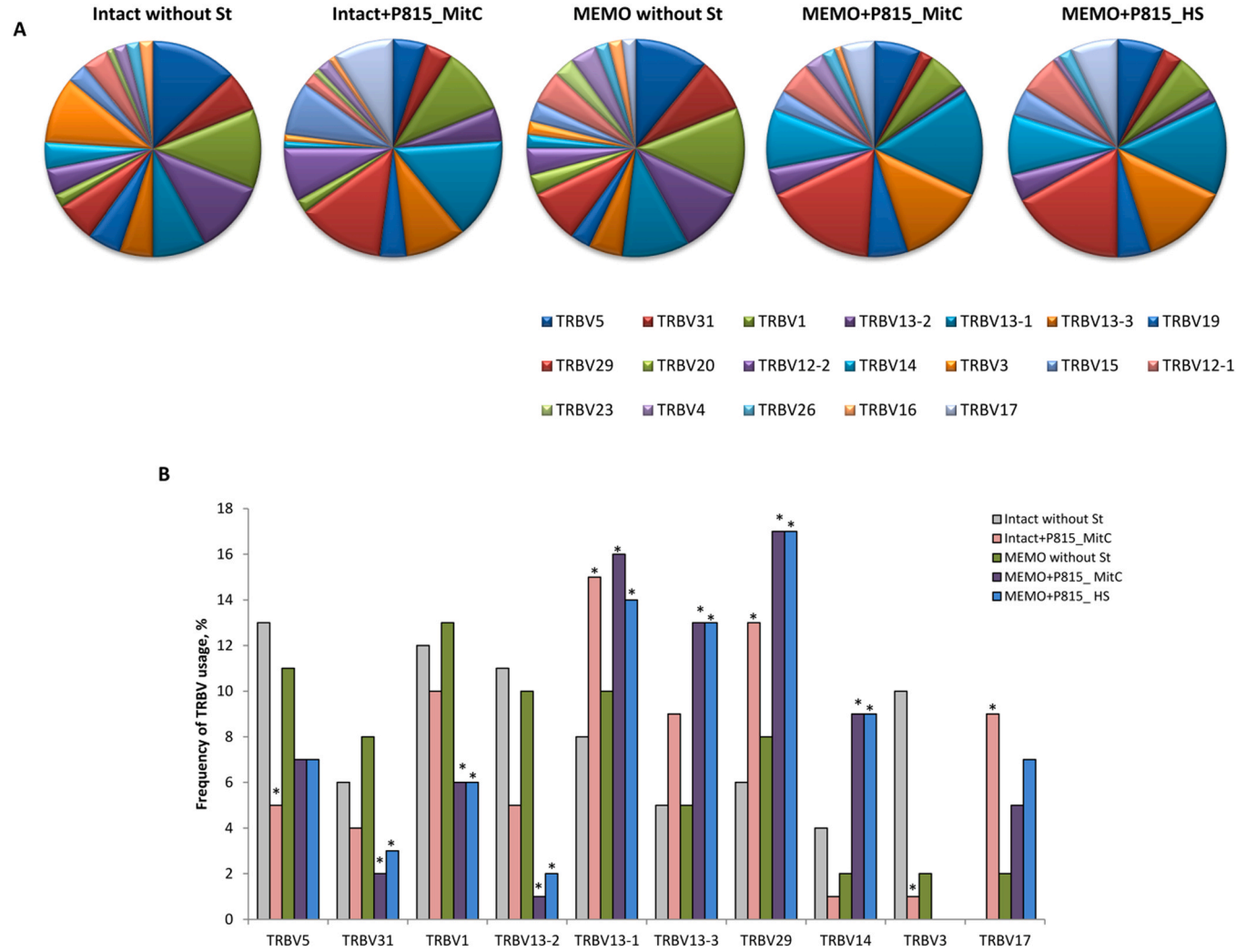

Fig. 2. Utilization of TRBV gene segments in the TOP-100 clonotypes of intact and P815-immunized mice after in vitro stimulation with P815. Splenocytes of the non-immunized (intact) or P815-immunized (MEMO) C57BL/6 mouse were cultured in vitro for 72 h without stimulation (without St) or with mastocytoma P815 cells treated with mitomycin C (P815_MitC) or acute heat shock (P815_HS). TCRα and TCRβ repertoires were then generated for each culture group. **A)** The use of TRBV gene segments (%) in the TOP-100 largest clonotypes in the repertoires of the intact and MEMO mice with and without in vitro stimulation. **B)** The discrepant use of individual TRBV gene segments (%) in the TOP-100 largest clonotypes in the repertoires of the intact and MEMO mice after in vitro stimulation. * $p < 0.05$ (Mann-Whitney U-test for comparison Intact+P815_MitC vs. Intact without St; Kruskal-Wallis test and Dunn's test for comparisons: MEMO+P815_MitC vs. MEMO without St and MEMO+P815_HS vs. MEMO without St).

3. Results

3.1. The TCRα and TCRβ repertoire diversity changed markedly during the secondary immune response to mastocytoma P815

To analyze changes in the TCR repertoire during the immune response to mastocytoma P815, we evaluated TCRα and TCRβ clonotype diversity in the repertoires of non-immunized (intact) and P815-immunized (MEMO) individual mice with or without in vitro stimulation with P815 (Table 1). The Shannon-Wiener diversity index and the Chao1 index were also calculated in each repertoire to assess clonality and diversity, respectively (Table 1). As these parameters strongly depend on the total count of identified clonotypes, which is different in each experimental group (Table 1), all repertoires were normalized by downsampling to an equal UMI count.

The primary in vitro immune response to P815 didn't change the diversity of both TCRα and TCRβ repertoires compared to the respective initial repertoires of the intact mouse (Table 1). In TCRα and TCRβ MEMO repertoires, the diversity and the number of unique clonotypes were 1.2- and 1.4-fold decreased, respectively, compared to the repertoires of the intact mouse without stimulation (Table 1). The minor decrease in Shannon-Wiener indices indicated a slight increase in clonality in the TCRα/β repertoires of the MEMO mouse. As expected, this confirmed that immunization of mice with mastocytoma P815 drove the establishment and expansion of memory T cell clonotypes.

In vitro re-challenge of T cells from the MEMO mouse with P815 dramatically decreased the TCR repertoire diversity compared to the MEMO repertoire without stimulation: 2.2- and 2.5-fold for TCRα and TCRβ repertoires, respectively (Table 1). Furthermore, the numbers of unique clonotypes in TCRα and TCRβ repertoires were 4.0- and 5.0-fold lower, respectively, vs. the initial MEMO repertoires. These indicated significant expansion of T cell clones during the secondary immune response. Notably, the diversity of TCRα/β MEMO repertoires was similar after re-stimulation of memory T cell with MitC- or HS-treated P815.

3.2. Discrepant usage of TRAV and TRBV gene segments by clonotypes involved in the primary and secondary immune responses to mastocytoma P815

To further estimate differences in the TCR repertoires during the primary and secondary immune responses to P815, the frequency of clonotypes with various TRAV and TRBV gene segments was evaluated for the TOP-100 largest clonotypes in each analyzed repertoire (Fig. 1, Fig. 2).

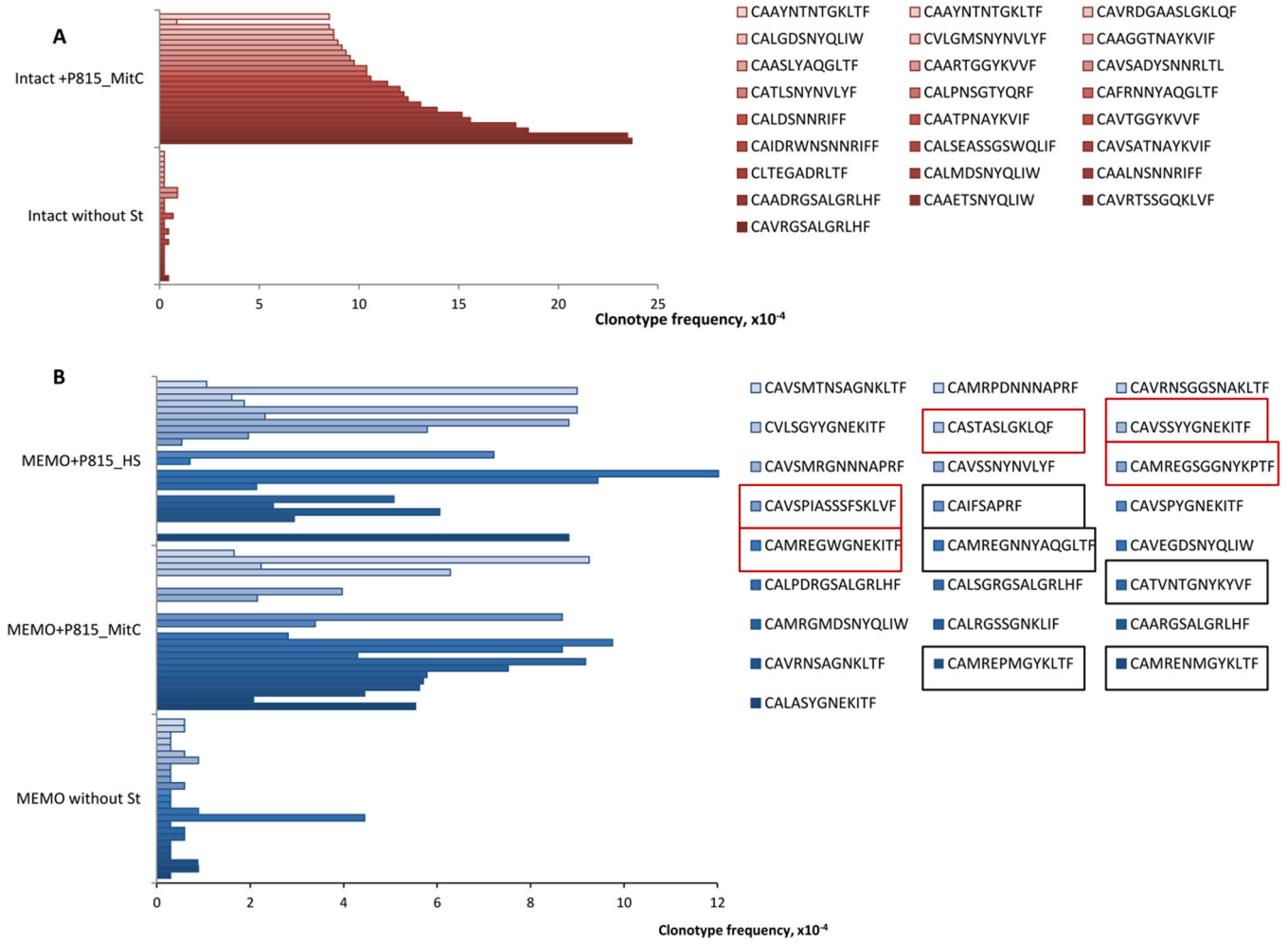

Fig. 3. TCRα clonotype expansion during the immune response to mastocytoma P815. TCRα/β repertoires of the non-immunized (intact) or P815-immunized (MEMO) C57BL/6 mouse were generated as described in Materials and methods. The frequencies of the TOP-25 largest TCRα clonotypes of the intact mouse (A) and the MEMO mouse (B) after co-culture with P815 were compared with the respective frequencies in the initial repertoire of the same intact or MEMO mouse without stimulation. MEMO clonotypes expanded only in response to P815_MitC or P815_HS are marked in black and red boxes, respectively.

In vitro P815 stimulation of T cells from the intact mouse didn't significantly alter the diversity and usage of TRAV gene segments compared to the initial repertoire of this intact mouse without stimulation (Fig. 1 A). Utilization of only TRAV12–3 was 6.0-fold increased in the TCRα repertoire of primarily activated effectors (Fig. 1B). Despite some reshaping of the TRAV usage in MEMO clonotypes, their Vα repertoire was very similar to that of the intact mouse with and without stimulation (Fig. 1 A,B). Re-stimulation of T lymphocytes from the MEMO mouse with P815 changed the TRAV utilization, significantly increasing the frequency of clonotypes with TRAV12D-3 (9.0–10.0-fold), TRAV12D-2 (4.0-fold), and TRAV3D-3 (6.0-fold) (Fig. 1B).

Interestingly, the primary immune response reshaped the utilization of Vβ gene segments compared to the initial repertoire of the intact mouse without stimulation (Fig. 2 A,B), significantly increasing the frequency of clonotypes with TRBV17 (9.0 vs. 0%), TRBV29 (13.0 vs. 6.0%), and TRBV13–1 (15.0 vs. 8.0%), while declining the relative counts of clonotypes with TRBV3 (1.0 vs. 10%) and TRBV5 (5.0 vs. 13.0%) (Fig. 2B). The TRBV repertoire of the MEMO mouse was very similar to that of the intact mouse without stimulation (Fig. 2). *In vitro* re-challenge of T cells of the MEMO mouse with P815 resulted in significant biases in the utilization of four Vβ gene segments: TRBV29 (17.0 vs. 8.0%), TRBV13–1 (14–16.0 vs. 10.0%), TRBV13–3 (13.0 vs. 5.0%), and TRBV14 (9.0 vs. 2.0%), with a decrease in the frequency of utilization of three gene segments: TRBV31 (2.0–3.0 vs. 8.0%), TRBV1 (6.0 vs. 13.0%), and TRBV13–2 (1.0 vs. 10.0%) vs. the initial MEMO repertoire (Fig. 2B). Notably, re-stimulation of T cells from the MEMO mouse with MitC- or HS-treated P815 resulted in similar changes in the utilization of Vα/β gene segments (Fig. 1, Fig. 2).

3.3. Unique clonotype expansion after in vitro antigenic stimulation of antigen-inexperienced and memory T cells

Co-culture of lymphocytes from both intact and MEMO mice with P815 induced the expansion of diverse TCRα (Fig. 3) and TCRβ (Fig. 4) clonotypes, whose frequencies increased three standard deviations above the frequency of the respective clonotype in the repertoire of unstimulated cells. The repertoires of such enriched TCRα/β clonotypes after antigenic stimulation significantly differed between intact and MEMO mice, with only 74 TCRα and 71 TCRβ common clonotypes observed (Fig. 5).

Importantly, the TCRαβ clonotype frequencies of enriched primarily activated effectors were markedly higher than the frequencies of expanded reactivated MEMO TCRαβ clonotypes (Fig. 3, Fig. 4), presumably implying that originally dominant clonotypes were mostly involved in the primary immune response. To evaluate the initial abundance of clonotypes, we calculated the probability of CDR3 generation (Pgen) for the TOP-25 largest TCRα and TCRβ clonotypes expanded after primary and secondary in vitro antigenic stimulation (Fig. 3, Fig. 4), assuming that Pgen characterizes not only the probability of CDR3 stochastic generation but also its belonging

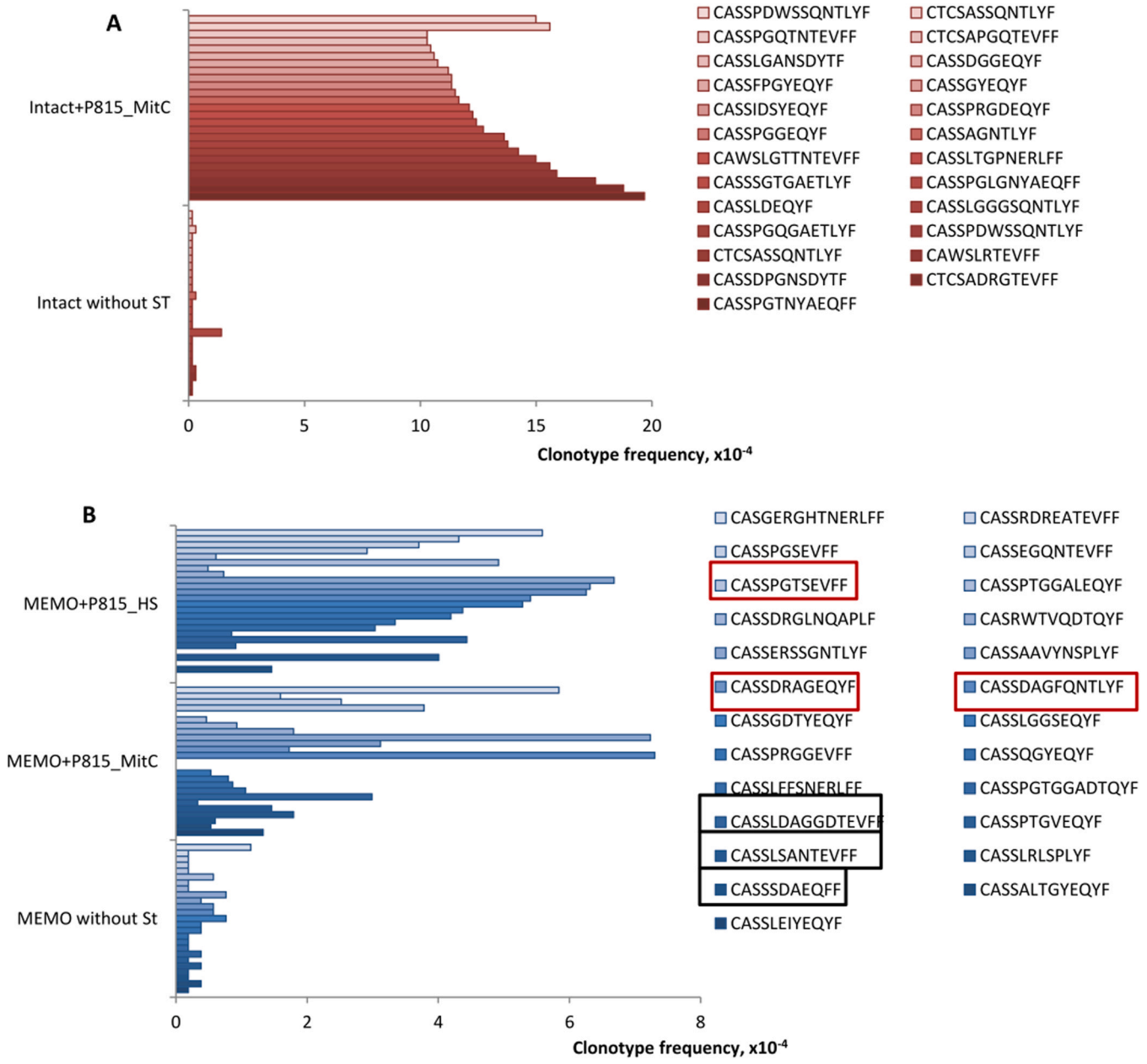

Fig. 4. TCRβ clonotype expansion during the immune response to mastocytoma P815. TCRα/β repertoires of the non-immunized (intact) or P815-immunized (MEMO) C57BL/6 mouse were generated as described in Materials and methods. The frequencies of the TOP-25 largest TCRβ clonotypes of the intact mouse (A) and the MEMO mouse (B) after co-culture with P815 were compared with the respective frequencies in the initial repertoire of the same intact or MEMO mouse without stimulation. MEMO clonotypes expanded only in response to P815_MitC or P815_HS are marked in black and red boxes, respectively.

to the functional repertoire. For TCRα and TCRβ clonotypes expanded after primary antigenic stimulation (Fig. 3A, Fig. 4A), Pgen ranged from 8.0×10^{-9} to 7.0×10^{-6} (median 1.9×10^{-6}) and from 7.0×10^{-8} to 8.0×10^{-6} (median 2.4×10^{-6}), respectively (Supplementary Fig. 3A, Supplementary Fig. 4A). For the enriched reactivated MEMO clonotypes (Fig. 3B, Fig. 4B), Pgen ranged from 8.0×10^{-10} to 7.0×10^{-6} (median 5.7×10^{-7}) for TCRα clonotypes (Supplementary Fig. 3B) and from 1.3×10^{-11} to 5.0×10^{-6} (median 1.9×10^{-7}) for TCRβ clonotypes (Supplementary Fig. 4B). This could indicate that initially abundant clonotypes with a high Pgen were predominantly expanded in a pool of antigen-inexperienced T cells after primary antigenic stimulation, while the cognate antigenic re-challenge of memory T cells drove selective expansion of more unique antigen-specific TCRαβ clonotypes that had mostly a low Pgen.

Interestingly, the TCRα/β MEMO repertoires were not identical after co-culture with MitC- or heat shock-treated P815, although they shared many common clonotypes (Fig. 5). We observed various expansion profiles of TCRα (Fig. 3B) and TCRβ (Fig. 4B) MEMO clonotypes depending on the stimulation conditions. Furthermore, distinct α/β memory clonotypes expanded only in response to P815_MitC (Fig. 3B, Fig. 4B, black boxes) or P815_HS (Fig. 3B, Fig. 4B, red boxes).

3.4. Prominent physicochemical characteristics of CDR3α of clonotypes involved in the secondary immune response to mastocytoma P815

The physicochemical properties of the CDR3 region of TCRα/β were evaluated for the TOP-100 largest clonotypes in each repertoire using VDJtools [28] (Supplementary Fig. 2) (Table 2).

No significant differences were detected for the CDR3 regions of both TCRα and TCRβ clonotypes in the repertoires of the intact mouse and the MEMO mouse without stimulation (Table 2, Fig. 6, Supplementary Fig. 5).

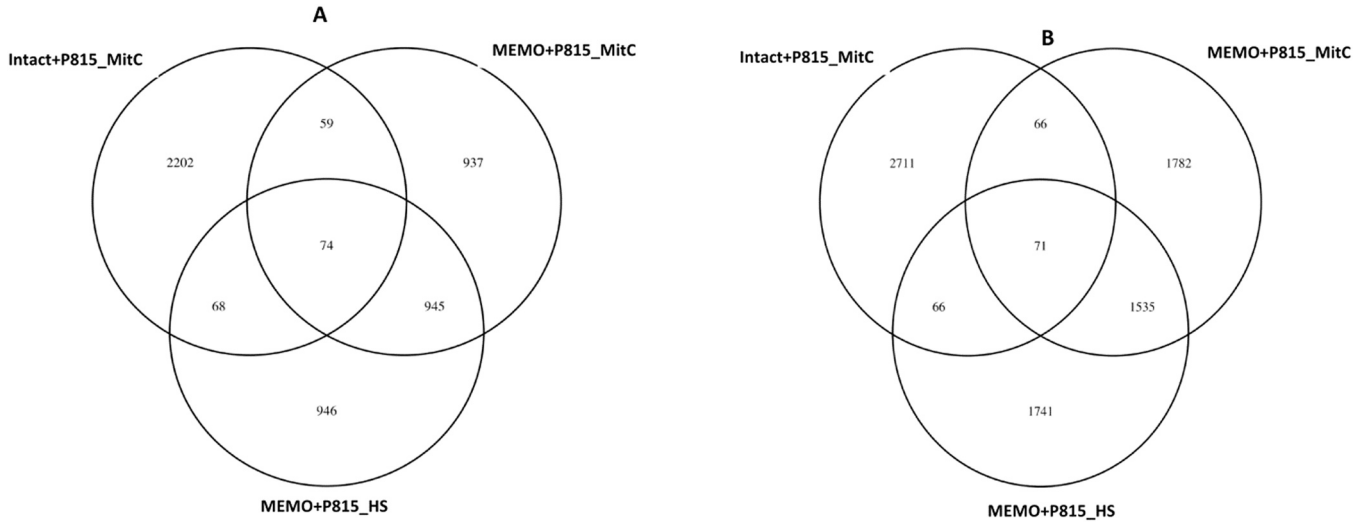

Fig. 5. TCRαβ repertoires of intact and P815-immunized mice share common enriched clonotypes after the immune response to mastocytoma P815. TCRα and TCRβ repertoires of the non-immunized (intact) or P815-immunized (MEMO) C57BL/6 mouse were generated after lymphocytes were cultured in vitro without stimulation or with mastocytoma P815 treated with mitomycin C (P815_MitC) or acute heat shock (P815_HS). The TCRα/β repertoires of the intact mouse and the MEMO mouse were compared pairwise to identify enriched clonotypes with significantly increased frequencies after antigenic stimulation. Comparative analysis of these enriched clonotypes in the stimulated repertoires of the intact and MEMO mice revealed unique and common TCRα (A) and TCRβ (B) clonotypes.

In the TCRα repertoire of the intact mouse after primary in vitro stimulation with P815, only the CDR3α interaction strength was significantly increased compared to this value in the initial repertoire of this mouse (Table 2A). Similarly, both conditions of in vitro re-stimulation of T lymphocytes from the MEMO mouse resulted in a significantly increased CDR3α strength compared to clonotypes in the repertoire of this MEMO mouse without stimulation (Table 2A, Fig. 6 A). Notably, 1% of re-stimulated MEMO clonotypes had a maximal CDR3α strength value equal to 11 (Fig. 6 A). Furthermore, CDR3α hydropathy increased 1.6-fold in re-stimulated MEMO clonotypes vs. MEMO clonotypes without stimulation (Table 2A, Fig. 6B). The total charge of the CDR3 region in TCRα MEMO clonotypes after P815 stimulation decreased 1.7-fold compared to the respective values in the initial MEMO repertoire and in the stimulated repertoire of the intact mouse (Table 2A, Fig. 6 C). This resulted from the increased frequency of neutral and negatively charged AAs in CDR3α of reactivated memory clonotypes (Fig. 6 C). We also detected a significantly increased CDR3α volume in the TCRα repertoire of the MEMO mouse after re-stimulation with MitC-treated P815 cells (Table 2A).

Analysis of the TCRβ physicochemical properties revealed only a significantly decreased strength of CDR3β in the repertoire of re-stimulated MEMO clonotypes (Table 2B). Other parameters of CDR3β were not changed for clonotypes of either intact or MEMO mice after in vitro P815 stimulation (Table 2B, Supplementary Fig. 5).

3.5. The physicochemical properties of the five central amino acids in CDR3 of TCRα and TCRβ clonotypes after primary and secondary P815 stimulation

Five central AAs of CDR3 often contact the presented antigen [30], and their physicochemical characteristics could influence the

Table 2
The physicochemical properties of CDR3α (A) and CDR3β (B) of the TOP-100 most frequent clonotypes in the repertoires of the non-immunized (intact) and P815-immunized (MEMO) C57BL/6 mouse with or without in vitro stimulation with mastocytoma P815 (mean ± SEM).

A)Parameter	Experimental group				
	Intact without St	Intact+P815_MitC	MEMO without St	MEMO+P815_MitC	MEMO+P815_HS
Length, aa	13.5 ± 0.1	13.4 ± 0.2	13.5 ± 0.1	13.7 ± 0.2	13.4 ± 0.2
Strength	5.07 ± 0.1	5.4 ± 0.1 *	4.95 ± 0.1	5.61 ± 0.1[#]	5.45 ± 0.1[#]
Hydropathy	3.4 ± 0.6	4.6 ± 0.6	2.6 ± 0.6	4.1 ± 0.7[¶]	4.1 ± 0.7[¶]
Charge	0.8 ± 0.09	0.6 ± 0.1	0.65 ± 0.08	0.38 ± 0.1[$]	0.39 ± 0.1[$]
Volume	1317.2 ± 11.3	1285.4 ± 16.4	1319.2 ± 15.6	1373.4 ± 17.8[¶]	1335.6 ± 19.1
Polarity	0.41 ± 0.008	0.41 ± 0.008	0.42 ± 0.009	0.42 ± 0.008	0.41 ± 0.008
B)Parameter	**Experimental group**				
	Intact without St	**Intact+P815_MitC**	**MEMO without St**	**MEMO+P815_MitC**	**MEMO+P815_HS**
Length, aa	13.7 ± 0.15	13.3 ± 0.16	13.7 ± 0.14	13.3 ± 0.16	13.3 ± 0.15
Strength	4.5 ± 0.1	4.5 ± 0.09	4.8 ± 0.1	**4.5 ± 0.1**[§]	**4.4 ± 0.1**[§]
Hydropathy	-3.4 ± 0.7	-2.5 ± 0.6	-2.9 ± 0.7	-4.1 ± 0.7	-3.4 ± 0.7
Charge	-0.91 ± 0.1	-0.82 ± 0.09	-0.83 ± 0.09	-0.84 ± 0.1	-0.94 ± 0.1
Volume	1316.9 ± 15.1	1285.4 ± 16.4	1335.9 ± 15.6	1280.7 ± 20.2	1290.5 ± 16.4
Polarity	0.52 ± 0.01	0.51 ± 0.01	0.51 ± 0.01	0.55 ± 0.01	0.54 ± 0.01

[*] $p < 0.05$ for comparison Intact+P815_MitC vs. Intact without St (Wilcoxon signed-rank test)
[#] $p < 0.01$ for comparisons MEMO+P815_MitC vs. MEMO without St and MEMO+P815_HS vs. MEMO without St (Wilcoxon signed-rank test)
[¶] $p < 0.05$ for comparisons MEMO+P815_MitC vs. MEMO without St and MEMO+P815_HS vs. MEMO without St (Wilcoxon signed-rank test);
[$] $p < 0.05$ for comparisons MEMO+P815_MitC vs. MEMO without St and MEMO+P815_HS vs. MEMO without St (Wilcoxon signed-rank test); MEMO+P815_MitC vs. Intact +P815_MitC and MEMO+P815_HS vs. Intact+P815_MitC (Kruskal-Wallis test)
[§] $p < 0.05$ for comparisons MEMO+P815_MitC vs. MEMO without St and MEMO+P815_HS vs. MEMO without St (Wilcoxon signed-rank test)

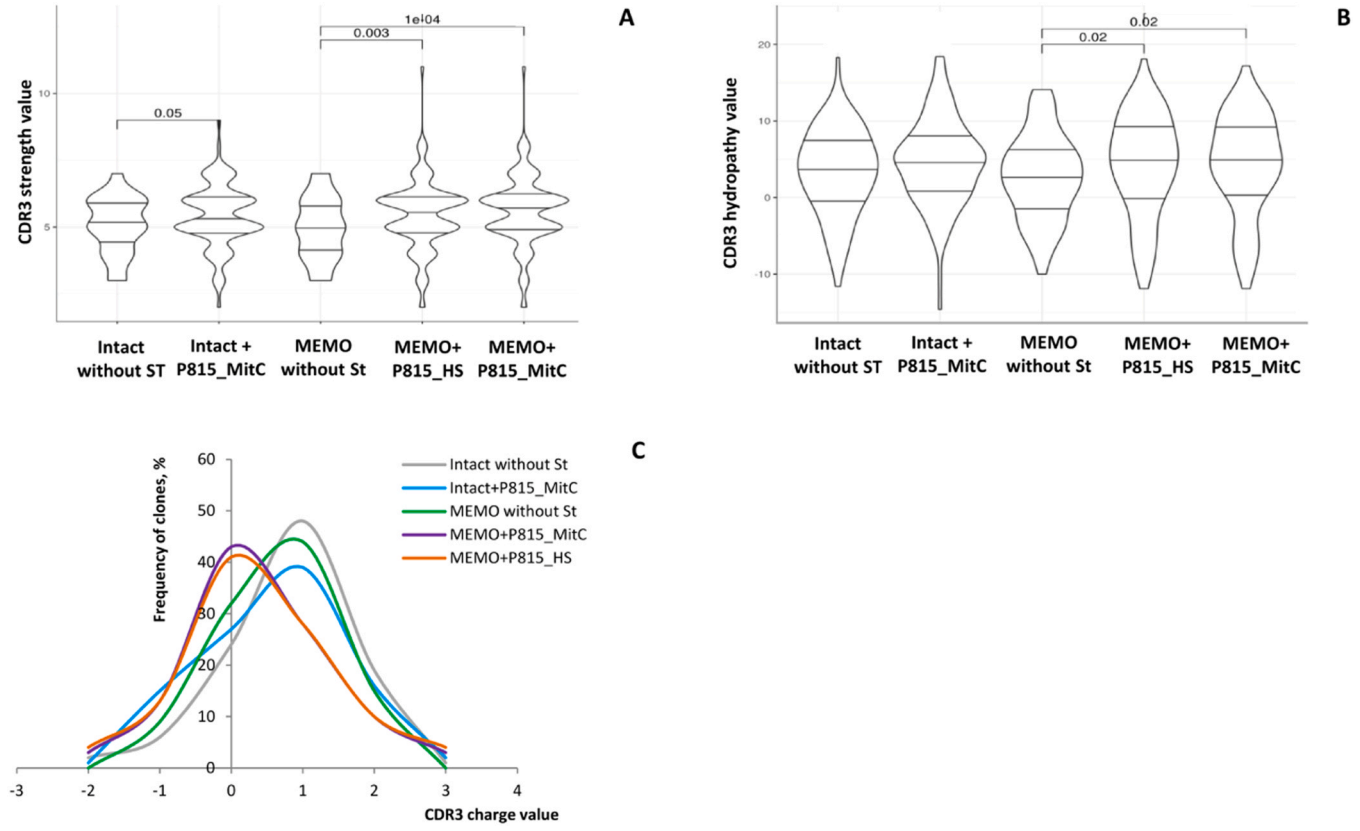

Fig. 6. Physicochemical properties of CDR3α in clonotypes of intact and P815-immunized mice after the response to mastocytoma P815. TCRα/β repertoires of the non-immunized (intact) or P815-immunized (MEMO) C57BL/6 mouse were generated as described in Materials and methods. The interaction strength (A), hydropathy (B), and charge (C) of the full CDR3α were evaluated using VDJtools for the TOP-100 most frequent clonotypes in each repertoire. The Mann-Whitney U-test and the Dunn's test were used to compare the repertoires of the intact mouse and the MEMO mouse, respectively.

properties of the whole CDR3 region. Thus, next, we analyzed the AA distribution among the five central residues of CDR3 (cCDR3) of the TOP-100 most frequent TCRα (Fig. 7 A) and TCRβ (Fig. 8 A) clonotypes in each repertoire. The frequencies of strongly interacting (Fig. 7B, Fig. 8B) and hydrophobic AAs (Fig. 7 C, Fig. 8 C) in cCDR3α and cCDR3β were also calculated. According to the Shannon entropy, the AA diversity in cCDR3α and cCDR3β was comparable in all analyzed repertoires (Supplementary Fig. 6 A, Supplementary Fig. 7 A).

cCDR3α of clonotypes in the initial repertoires of the intact mouse and the MEMO mouse without in vitro antigenic stimulation showed no significant differences in their physicochemical parameters (Fig. 7). Comparative analysis of cCDR3α in the TCRα repertoires of the intact mouse showed that after P815 stimulation, cCDR3α had a slightly (1.2-fold) increased frequency of strongly interacting AAs (Fig. 7B) and a 1.4-fold increased rate of hydrophobic AAs (Fig. 7 C). Re-distribution of strongly interacting AAs (F, I, L, M, V, W, and Y) within cCDR3α of primarily stimulated effector clonotypes was also observed, with elevated rates at cCDR3α positions 1 and 3 compared to clonotypes of the intact mouse without stimulation (Fig. 7 A, Supplementary Fig. 6B).

Similarly, in the TCRα repertoire of MEMO clonotypes after in vitro re-stimulation, cCDR3α contained a 1.3–1.5-fold greater rate of strongly interacting AAs vs. cCDR3α of MEMO clonotypes without re-stimulation (Fig. 7B). The increased utilization of strongly interacting AAs at positions 2 and 3 of cCDR3α resulted in their even distribution throughout cCDR3α of re-stimulated MEMO clonotypes (Fig. 7 A, Supplementary Fig. 6B). Furthermore, after re-stimulation by heat shock-treated P815, cCDR3α of MEMO clonotypes had a 1.3-fold higher frequency of hydrophobic AAs (Fig. 7 C) with the median hydropathy tending to increase 1.4-fold compared to the respective values for cCDR3α in the initial MEMO repertoire (Fig. 7D).

When compared to cCDR3β of clonotypes in the repertoire of the intact mouse without stimulation (Fig. 8 A, Supplementary Fig. 7B), the central part of CDR3β of unstimulated MEMO clonotypes contained a 1.3-fold increased frequency of strongly interacting AAs, primarily at positions 2 and 5 (Fig. 8 A, B). No significant changes were detected in the physicochemical properties of cCDR3 of TCRβ clonotypes after in vitro stimulation of T lymphocytes from either intact or MEMO mice compared to the respective initial repertoires (Fig. 8). Still, we observed some re-distribution of strongly interacting AAs in cCDR3β of clonotypes after the primary and secondary in vitro antigenic challenges (Fig. 8 A, Supplementary Fig. 7B). TCRβ clonotypes of primarily activated effectors had a 2.0-fold higher frequency of strongly interacting AAs at position 4 of cCDR3β than clonotypes from the initial repertoire of the intact mouse (Fig. 8 A, Supplementary Fig. 7B). Reactivated TCRβ MEMO clonotypes contained strongly interacting AAs more frequently at positions 1 and 5 of their cCDR3 compared to cCDR3β of MEMO clonotypes without stimulation (Fig. 8 A, Supplementary Fig. 7B).

3.6. Features of the CDR1 and CDR2 regions of TCRα and TCRβ memory clonotypes changed notably after the cognate antigenic re-stimulation

Previously, we showed that memory T cells predominantly execute direct recognition in allogeneic recognition [31], presuming TCR interactions with allogeneic MHC molecules. As the CDR1 and CDR2 regions primarily make contacts with MHC [2], next we sought to analyze the physicochemical properties of these loops in clonotypes involved in the primary and secondary immune responses to mastocytoma P815. Since CDR1 and CDR2 are encoded by the V segment and their diversity is limited by the germ-line gene segments available for recombination [32,33], we evaluated the strength and

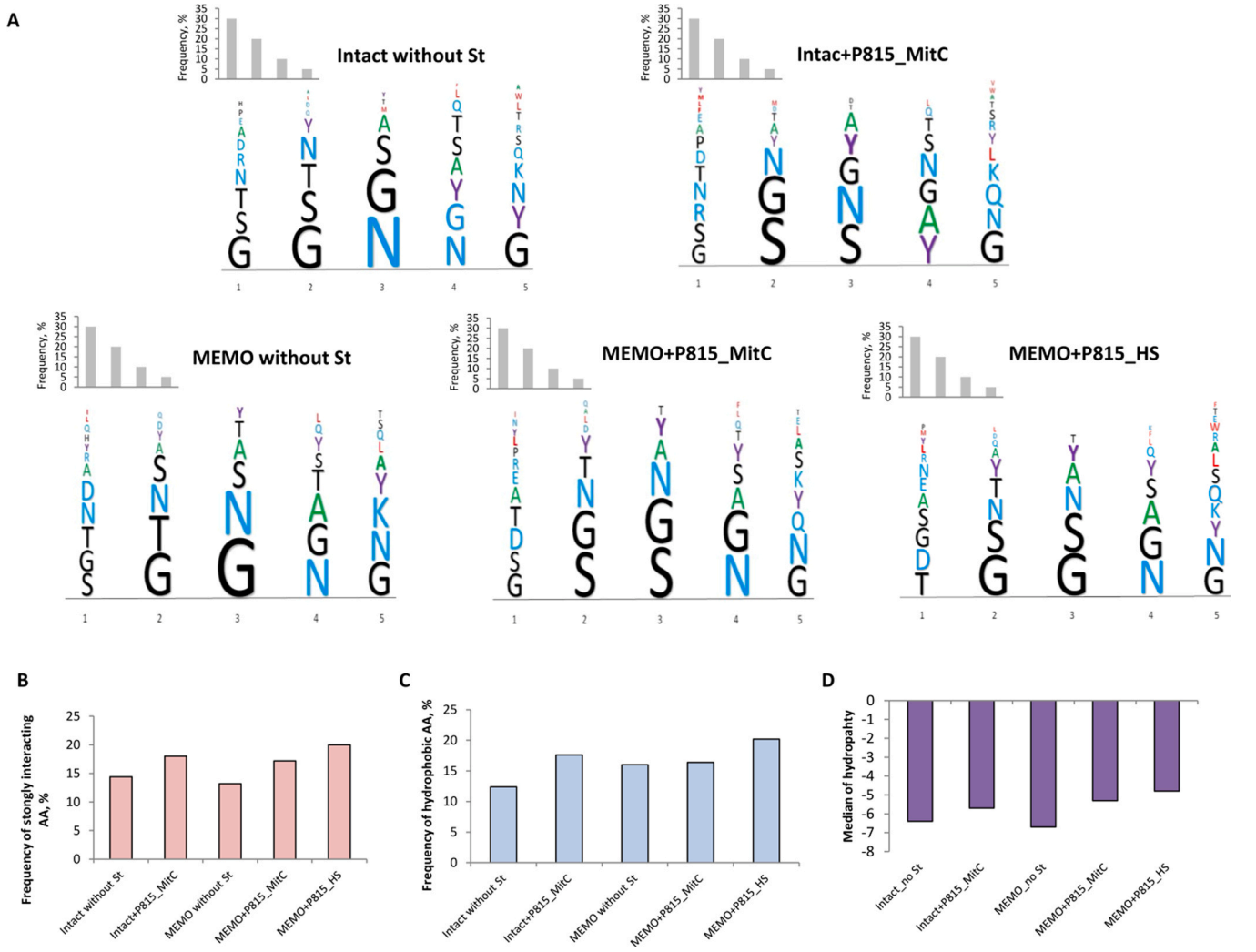

Fig. 7. Physicochemical properties of the five central amino acids of CDR3α in clonotypes of intact and P815-immunized mice after the response to mastocytoma P815. TCRα/β repertoires of the non-immunized (intact) or P815-immunized (MEMO) C57BL/6 mouse were generated as described in Materials and methods. A) The distribution of amino acids (AAs) (black - neutral, blue - hydrophilic, green - hydrophobic, red - strongly interacting hydrophobic, violet - strongly interacting neutral) was analyzed for the five central positions of CDR3α (cCDR3α) in the TOP-100 most frequent clonotypes in each generated repertoire. The utilization (%) of strongly interacting AAs (B), hydrophobic AAs (C), and the median hydropathy (D) were calculated for cCDR3α of the TOP-100 clonotypes in each repertoire.

hydropathy of TRAV-germ and TRBV-germ for the TOP-100 largest clonotypes in the repertoire of the intact mouse and the MEMO mouse with and without stimulation (Fig. 9).

The V-germ strength tended to increase in MEMO TCRα clonotypes after in vitro re-stimulation, while it declined in stimulated MEMO TCRβ clonotypes compared to the respective initial MEMO repertoires (Fig. 9A). The V-germ hydropathy of reactivated MEMO TCRα/β clonotypes showed the opposite trend (Fig. 9B). Unstimulated TCRα/β clonotypes of the MEMO mouse showed no significant differences in these parameters when compared to unstimulated clonotypes of the intact mice (Fig. 9). *In vitro* primary stimulation of T cells from the intact mouse resulted only in a drop in the mean TRAV-germ hydropathy without affecting its strength or TRBV-germ parameters.

4. Discussion

In this study, we aimed to track sequential changes in the TCRαβ repertoire during the immune response to the allogeneic tumor in mice, starting from the primary response to the formation of immunological memory and the induction of the secondary immune response of memory cells. For this, we exploited the experimental system that involves the cognate antigenic in vitro re-stimulation of long-lived memory T cells established in the course of the primary immune response to tumor alloantigens in vivo [18,20]. Our functional assay is advantageous because it allows us to generate and characterize a selective pool of functionally true antigen-specific memory T cells. The features of TCRαβ repertoires of reactivated memory T cells were compared to those of primarily activated effectors.

In vitro co-culture of lymphocytes from a non-immunized mouse with allogeneic mastocytoma P815 induced expansion of various TCRα and TCRβ clonotypes without, however, affecting the total clonotype diversity or the number and size of unique clonotypes. Only the biased utilization of concrete Vα/β gene segments and the increased interaction strength of CDR3α were detected for effector clonotypes expanded during the primary response. Other physicochemical properties of the CDR3 region in TCRα and TCRβ clonotypes remained unchanged after primary stimulation by P815. This data suggested a polyclonal T cell response after the first antigen encounter, involving effectors with diverse TCR features, including variable affinities [34,35].

As expected, some decline in the TCRα and TCRβ clonotype diversity was found in the repertoire of the P815-immunized mouse

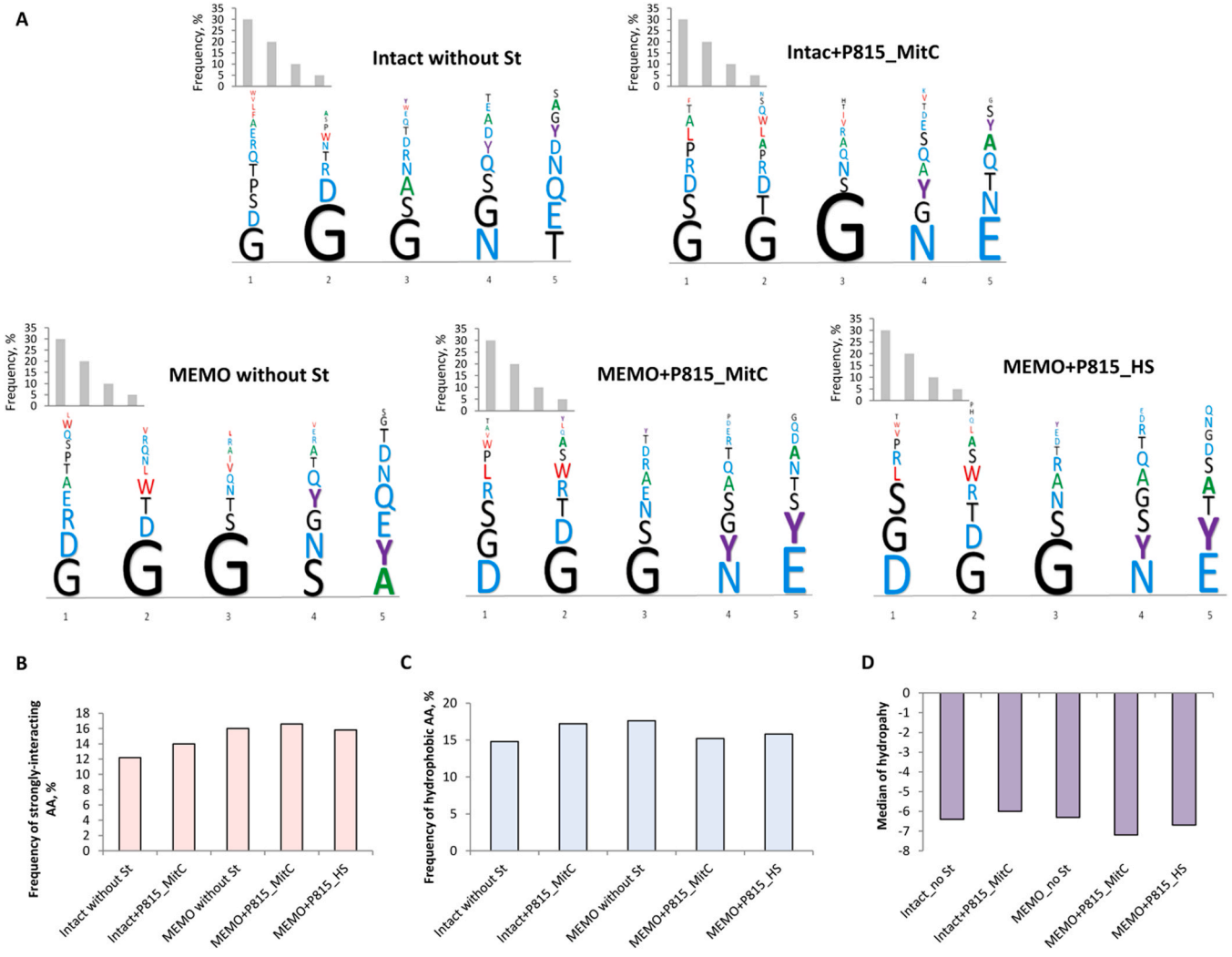

Fig. 8. Physicochemical properties of the five central amino acids of CDR3β in clonotypes of intact and P815-immunized mice after the response to mastocytoma P815. TCRα/β repertoires of the non-immunized (intact) or P815-immunized (MEMO) C57BL/6 mouse were generated as described in Materials and methods. A) The distribution of amino acids (AAs) (black - neutral, blue - hydrophilic, green - hydrophobic, red - strongly interacting hydrophobic, violet - strongly interacting neutral) was analyzed for the five central positions of CDR3β (cCDR3β) in the TOP-100 most frequent clonotypes in each generated repertoire. The utilization (%) of strongly interacting AAs (B), hydrophobic AAs (C), and the median hydropathy (D) were calculated for cCDR3β of the TOP-100 clonotypes in each repertoire.

(Table 1), suggesting the formation of long-lived memory T cells in the course of the primary in vivo immune response to mastocytoma cells [18]. Still, the establishment of immunological memory didn't cause significant disturbances in the TCRαβ repertoire of the P815-immunized mouse compared to the repertoire of a non-immunized mouse (Figs. 1, 2, 3, and Supplementary Fig. 5). We assume that this could be due to the small size of long-lived memory clonotypes, which are maintained after the contraction of the primary immune response.

The cognate antigenic re-stimulation of T cells from the P815-immunized mouse induced significant clonotype expansion during the secondary immune response, resulting in a dramatic contraction of the TCRαβ repertoire diversity (Table 1). Importantly, expanded reactivated memory clonotypes had markedly lower frequencies and Pgen compared to those of enriched clonotypes of primarily activated effectors, implying that the secondary antigen encounter drove more selective expansion of unique antigen-specific clonotypes (Fig. 3, Fig. 4, Supplementary Fig. 3, and Supplementary Fig. 4). It is also worth noting that different TCRα and TCRβ clonotypes responded differently to stimulator P815 cells, whether treated with the cytostatic or exposed to acute heat shock. However, different stimulating conditions provoked similar changes in the features of TCRαβ repertoires of expanded memory clonotypes (Fig. 6, Fig. 9, and Supplementary Fig. 5).

Memory cells have a lower activation threshold than naive T cells [36,37] and rapidly acquire an effector state upon re-encounter with the antigen presented even at much lower doses [37–39]. It was also shown that memory T cells are relatively independent of co-stimulation from antigen-presenting cells (APCs) [20,23]. Therefore, in our experimental system, MitC-treated tumor cells could provide too strong stimuli to some memory clones, inducing activation apoptosis in them. In contrast, re-challenge of memory cells with heat shock-treated stimulators could provide more favorable conditions for their activation and expansion, as acute heat shock was shown to disturb the formation of the stable immunological synapse between a T cell and exposed cells [21,22] and to inhibit the expression of co-stimulatory molecules (specifically, the B7 ligand) on APCs [20]. We hypothesize that taking into account the physiological features of naive T cells, effectors, and memory T cells [37] may enhance the selectivity and specificity of activation and expansion of desired cell subsets using in vitro techniques.

Comparative bioinformatics analyses revealed significant changes in the physicochemical properties of CDR3α in clonotypes involved in the secondary immune response to allogeneic tumor

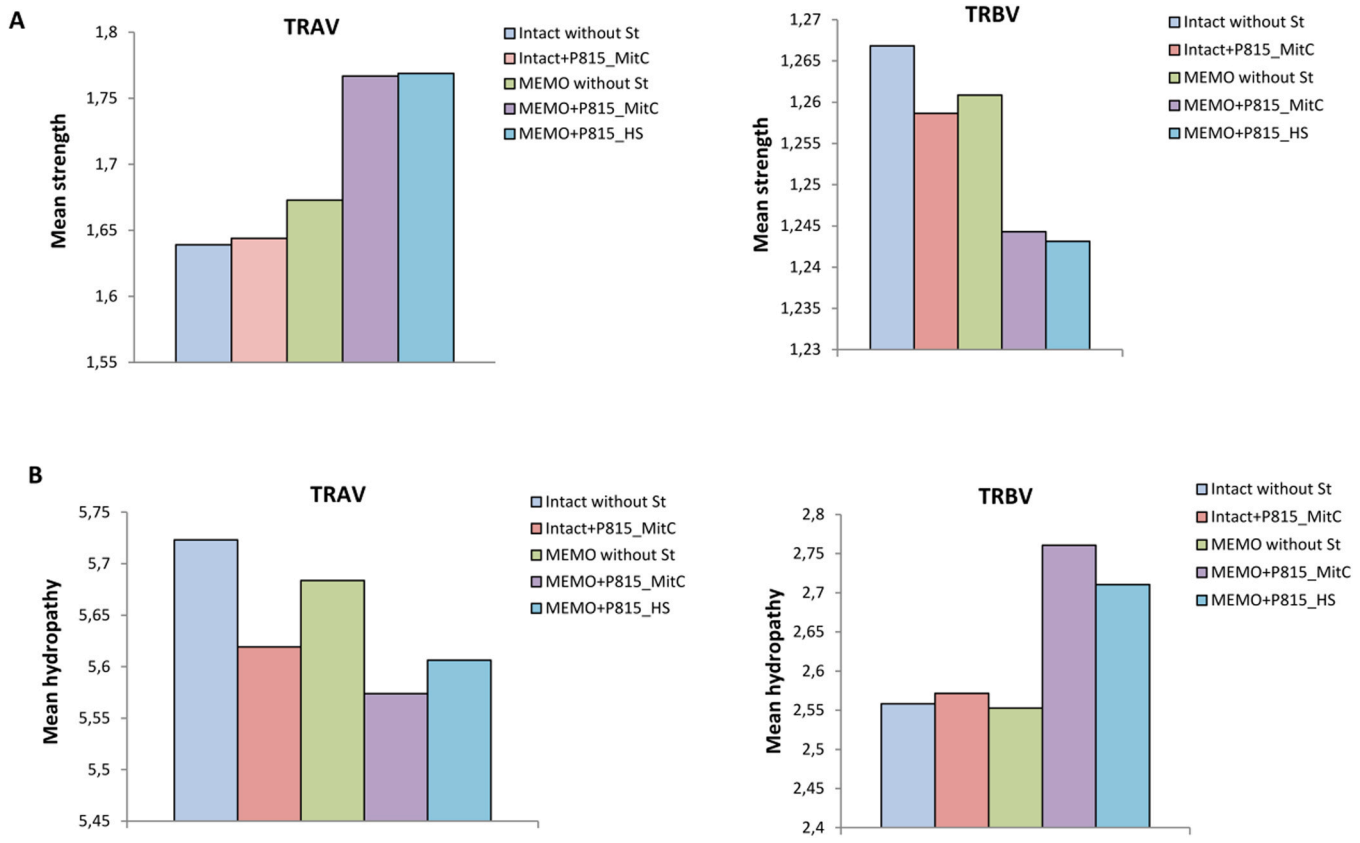

Fig. 9. Strength and hydropathy of CDR1 and CDR2 in TCRαβ clonotypes of intact and P815-immunized mice after the response to mastocytoma P815. TCRα/β repertoires of the non-immunized (intact) or P815-immunized (MEMO) C57BL/6 mouse were generated as described in Materials and methods. For the TOP-100 most frequent clonotypes in each generated TCRα and TCRβ repertoire, the strength of interaction (A) and hydropathy (B) of the Vα- and Vβ-germ segments were calculated.

cells. The CDR3 region of re-stimulated TCRα memory clonotypes became rich in hydrophobic, strongly interacting, and bulky amino acids (AAs) (Table 2). The same tendency toward abundance of strongly interacting and hydrophobic AAs was found in the middle part (the five central AAs) of these CDR3α that made major contacts with a presented peptide [30]. These findings were in agreement with more recent research by Kasatskaya et al., which demonstrated that certain functional subsets of human effector/memory T cells express TCRs with high numbers of hydrophobic and strongly interacting AAs within their CDR3αβ [17]. Such physicochemical signatures of the CDR3 region are believed to be associated with high cross-reactivity of TCR [40–42]. We also noted an even distribution of strongly interacting AAs within the five central residues of CDR3α of re-stimulated memory clonotypes, suggesting that their TCRs could require fewer important contacts to recognize a docked peptide [43]. These findings further supported the hypothesis of increased TCR cross-reactivity in memory clones elicited in the secondary immune response, which complied with our recent studies [31].

Along with the substantial narrowing of the TCR repertoire diversity and intense clonotype expansion, presumably high TCR cross-reactivity in re-stimulated memory clonotypes could point out that the secondary immune response drove the selection of more efficient clones capable of recognizing multiple tumor peptide antigens and emergent mutants. It seems plausible that such cross-reactive clonotypes could better control tumor cells with a high mutation rate. Accordingly, several studies indicated that cross-reactive TCRs controlled fast-mutating viruses more efficiently [43,44]. Furthermore, TCRs with poly-restriction to multiple antigens presented by different MHC alleles are proposed to be the most efficient for adoptive immunotherapy [7].

Interestingly, we also detected the tendency for an increasing interaction strength of the germ-line Vα segments of memory clonotypes expanded during the cognate antigenic re-stimulation (Fig. 9A). This could be associated with the observed biased utilization of certain TRAV gene segments by these clonotypes (Fig. 1). This is in line with the previous study that indicated different cumulative interaction strengths of CDR1 and CDR2 for various TRAV and TRBV [42]. Memory T cells rely mainly on direct recognition in the allogeneic immune response [31]. Therefore, the stronger CDR1 and CDR2 loops of re-stimulated TCRα memory clonotypes suggested the expansion of clones with α-chains that strongly bind to allogeneic MHC class I molecules (H2-K^d and H2-D^d) expressed on mastocytoma P815 cells.

Accordingly, in our experimental system, memory T cells that were activated and expanded during the secondary immune response expressed TCRα that strongly interacted with both MHC and docked peptides. Our results comply with other studies, which demonstrated that in the secondary response, T cells express TCRs with higher affinity for MHC-peptide complexes than those involved in the primary response [9,10]. This could reflect functional avidity maturation in antigen-experienced T cells [7,45,46].

Of particular note are our findings of minor changes in the CDR features of TCRβ memory clonotypes involved in the secondary immune response to P815 antigens. The observed decreased interaction strength of all three CDRs of TCRβ in re-stimulated memory clonotypes (Table 2B, Fig. 9A) could be a reciprocal effect of the increased CDRα strength, as also seen for some other physicochemical properties of TCRαβ [42,47]. Such disparities in TCRα and TCRβ CDR characteristics may indicate distinct roles for each hemi-chain in the secondary allogeneic immune response in our experimental system, implying that memory T cells relied mainly on TCRα in recognition of

the cognate alloantigens. Such asymmetric contribution of an α- and β-chain TCR in antigen recognition is known as TCR chain centricity [48,49]. In view of our earlier studies, which showed that some memory clones express chain-centric TCRs with a dominant-active antigen-specific α-chain [50,51], the indications here of the dominating function of TCRα in alloantigen recognition by memory T cells are especially interesting. The findings of the current research may aid in the ongoing improvement of the generation of TCR-modified T cell products based on TCR chain centricity, a novel approach for ACT proven to be efficient and safe in our experimental tumor and infectious mouse models [50–52].

In this study, we succeeded in clearly identifying important TCR characteristics of reactivated memory T cells by comparing the TCR repertoires of effectors involved in the primary immune response and memory T cells expanded during the cognate antigen re-encounter. It is hypothesized that the identified TCR characteristics may serve as a common signature for antigen-specific memory T cells, even though we only exploited one experimental tumor model here. A number of approaches based on TCR cluster analysis have been described to find clonotypes involved in the immune response in an unsorted T cell repertoire [13,14]. Results of this work could contribute to the development of bioinformatics strategies to specifically identify memory clonotypes in a bulk T cell repertoire based on the physicochemical properties of their TCRα/β. We assume that functionally true memory T cells enriched by in vitro cognate stimulation could be a better source of therapeutic TCRs for ACT with improved TCR-pMHC affinity interaction and cross-reactivity to multiple tumor antigens. Still, the specificity, efficacy, and safety of selected TCRs must be thoroughly evaluated in functional assays.

Funding

This work was supported by the grant of Russian Science Foundation #22–15–00342 (2022–2024).

CRediT authorship contribution statement

Anastasiia Kalinina: Conceptualization, Study design, Methodology, in vivo and *ex vivo* experiments, Formal analyses, Writing – original draft, Writing – review & editing, Visualization. **Nadezda Persiyantseva:** Formal analyses, Writing – review & editing, Visualization. **Olga Britanova**: Methodology, Generation of cDNA libraries, Bioinformatics analysis, Formal analyses, Resources, Writing – review & editing, Visualization. **Ksenia Lupyr:** Methodology, Generation of cDNA libraries, Bioinformatics analysis, Formal analyses, Writing – review & editing, Visualization. **Irina Shagina**: Methodology, Generation of cDNA libraries, Bioinformatics analysis. **Ludmila Khromykh**: Resources, Data curation, Writing – review & editing, Supervision, Project administration. **Dmitry Kazansky:** Conceptualization, Study design, Methodology, Resources, Data curation, Writing – review & editing, Supervision, Project administration, Funding acquisition. All authors read and approved the final manuscript.

Declaration of Competing Interest

The authors declare that they have no known competing financial interests or personal relationships that could have appeared to influence the work reported in this paper.

Appendix A. Supporting information

Supplementary data associated with this article can be found in the online version at doi:10.1016/j.csbj.2023.05.028.

References

[1] Fleit Howard. Janeway's Immunobiology by Kenneth Murphy, Charles A. Janeway, Paul Travers, Mark Walport, Allan Mowat, and Casey T. Weaver. Q Rev Biol 2012;87:266–7. https://doi.org/10.1086/666778
[2] Rudolph MG, Stanfield RL, Wilson IA. How TCRs bind MHCs, peptides, and coreceptors. Annu Rev Immunol 2006;24:419–66.
[3] D'Ippolito E, Schober K, Nauerth M, Busch DH. T cell engineering for adoptive T cell therapy: safety and receptor avidity. Cancer Immunol Immunother 2019;68:1701–12. https://doi.org/10.1007/s00262-019-02395-
[4] Wolf B, Zimmermann S, Arber C, Irving M, Trueb L, Coukos G. Safety and tolerability of adoptive cell therapy in cancer. Drug Saf 2019;42(2):315–34. https://doi.org/10.1007/s40264-018-0779-3
[5] Jiang T, Shi T, Zhang H, et al. Tumor neoantigens: from basic research to clinical applications. J Hematol Oncol 2019;12:93. https://doi.org/10.1186/s13045-019-0787-5
[6] Davis MM, Boniface JJ, Reich Z, Lyons D, Hampl J, Arden B, et al. Ligand recognition by alpha beta T cell receptors. Annu Rev Immunol 1998;16:523–44. https://doi.org/10.1146/annurev.immunol.16.1.523
[7] Hebeisen M, Allard M, Gannon PO, Schmidt J, Speiser DE, Rufer N. Identifying individual T cell receptors of optimal avidity for tumor antigens. Front Immunol 2015;6:582. https://doi.org/10.3389/fimmu.2015.00582
[8] Verdeil G, Fuertes Marraco SA, Murray T, Speiser DE. From T cell "exhaustion" to anti-cancer immunity. Biochim Biophys Acta 2016;1865(1):49–57. https://doi.org/10.1016/j.bbcan.2015.06.007
[9] Mondino A, Manzo T. To remember or to forget: the role of good and bad memories in adoptive T cell therapy for tumors. Front Immunol 2020;11:1915. https://doi.org/10.3389/fimmu.2020.01915
[10] Savage PA, Boniface JJ, Davis MM. A kinetic basis for T cell receptor repertoire selection during an immune response. Immunity 1999;10(4):485–92. https://doi.org/10.1016/s1074-7613(00)80048-5
[11] Busch DH, Fräßle SP, Sommermeyer D, Buchholz VR, Riddell SR. Role of memory T cell subsets for adoptive immunotherapy. Semin Immunol 2016;28(1):28–34. https://doi.org/10.1016/j.smim.2016.02.001
[12] Sommermeyer D, Hudecek M, Kosasih PL, Gogishvili T, Maloney DG, Turtle CJ, et al. Chimeric antigen receptor-modified T cells derived from defined CD8+ and CD4+ subsets confer superior antitumor reactivity in vivo. Leukemia 2016;30(2):492–500. https://doi.org/10.1038/leu.2015.247
[13] Pogorelyy MV, Minervina AA, Shugay M, Chudakov DM, Lebedev YB, Mora T, et al. Detecting T cell receptors involved in immune responses from single repertoire snapshots. PLoS Biol 2019;17(6):e3000314. https://doi.org/10.1371/journal.pbio.3000314
[14] Goncharov MM, Bryushkova EA, Sharaev NI, Skatova VD, Baryshnikova AM, Sharonov GV, et al. Pinpointing the tumor-specific T cells via TCR clusters. Elife 2022;11:e77274. https://doi.org/10.7554/eLife.77274
[15] Dash P, Fiore-Gartland AJ, Hertz T, Wang GC, Sharma S, Souquette A, et al. Quantifiable predictive features define epitope-specific T cell receptor repertoires. Nature 2017;547(7661):89–93. https://doi.org/10.1038/nature22383
[16] Glanville J, Huang H, Nau A, Hatton O, Wagar LE, Rubelt F, et al. Identifying specificity groups in the T cell receptor repertoire. Nature 2017;547(7661):94–8. https://doi.org/10.1038/nature22976
[17] Kasatskaya SA, Ladell K, Egorov ES, Miners KL, Davydov AN, Metsger M, et al. Functionally specialized human CD4$^+$ T-cell subsets express physicochemically distinct TCRs. Elife 2020;9:e57063. https://doi.org/10.7554/eLife.57063
[18] Grinenko TS, Pobezinskaya EL, Pobezinskii LA, Baturina IA, Zvezdova ES, Kazanskii DB. Suppression of primary allogenic response by CD8+ memory cells. Bull Exp Biol Med 2005;140(5):545–9. https://doi.org/10.1007/s10517-006-0020-8
[19] Kalinina AA, Khromykh LM, Kazansky DB, Deykin AV, Silaeva YY. Suppression of the immune response by syngeneic splenocytes adoptively transferred to sublethally irradiated mice. Acta Nat 2021;13(1):116–26. https://doi.org/10.32607/actanaturae.11252
[20] Kazansky Dmitry, Petrishchev V, Shtil A, Chernysheva Anna, Sernova Natalia, Abronina I, et al. Heat shock of antigen-presenting cells as a method for functional testing of the T cells of allospecific memory. Russ J Bioorg Chem 1999;25:99–109.
[21] Coss RA, Linnemans WA. The effects of hyperthermia on the cytoskeleton: a review. Int J Hyperth 1996;12(2):173–96. https://doi.org/10.3109/02656739609022507
[22] Al-Alwan MM, Rowden G, Lee TD, West KA. The dendritic cell cytoskeleton is critical for the formation of the immunological synapse. J Immunol 2001;166(3):1452–6. https://doi.org/10.4049/jimmunol.166.3.1452
[23] Watson AR, Lee WT. Differences in signaling molecule organization between naive and memory CD4+ T lymphocytes. J Immunol 2004;173(1):33–41. https://doi.org/10.4049/jimmunol.173.1.33
[24] Egorov ES, Merzlyak EM, Shelenkov AA, Britanova OV, Sharonov GV, Staroverov DB, et al. Quantitative profiling of immune repertoires for minor lymphocyte counts using unique molecular identifiers. J Immunol 2015;194(12):6155–63.
[25] Shugay M, Britanova OV, Merzlyak EM, Turchaninova MA, Mamedov IZ, Tuganbaev TR, et al. Towards error-free profiling of immune repertoires. Nat Methods 2014;11(6):653–5.
[26] Bolotin DA, Poslavsky S, Mitrophanov I, Shugay M, Mamedov IZ, Putintseva EV, et al. MiXCR: software for comprehensive adaptive immunity profiling. Nat Methods 2015;12(5):380–1.
[27] Mayer-Blackwell K, Schattgen S, Cohen-Lavi L, Crawford JC, Souquette A, Gaevert JA, et al. TCR meta-clonotypes for biomarker discovery with *tcrdist3* enabled identification of public, HLA-restricted clusters of SARS-CoV-2 TCRs. Elife 2021;10:e68605. https://doi.org/10.7554/eLife.68605

[28] Shugay M, Bagaev DV, Turchaninova MA, Bolotin DA, Britanova OV, Putintseva EV, et al. VDJtools: unifying post-analysis of T cell receptor repertoires. PLoS Comput Biol 2015;11(11):e1004503. https://doi.org/10.1371/journal.pcbi.1004503
[29] Stewart JJ, Lee CY, Ibrahim S, Watts P, Shlomchik M, Weigert M, et al. A Shannon entropy analysis of immunoglobulin and T cell receptor. Mol Immunol 1997;34(15):1067–82. https://doi.org/10.1016/s0161-5890(97)00130-2
[30] Egorov ES, Kasatskaya SA, Zubov VN, Izraelson M, Nakonechnaya TO, Staroverov DB, et al. The changing landscape of naive T cell receptor repertoire with human aging. Front Immunol 2018;9:1618. https://doi.org/10.3389/fimmu.2018.01618
[31] Pobezinskaya EL, Pobezinskii LA, Silaeva YY, Anfalova TV, Khromykh LM, Tereshchenko TS, et al. Cross reactivity of T cell receptor on memory CD8+ cells isolated after immunization with allogeneic tumor cells. Bull Exp Biol Med 2004;137(5):493–8. https://doi.org/10.1023/b:bebm.0000038162.13508.3a
[32] Stadinski BD, Trenh P, Smith RL, Bautista B, Huseby PG, Li G, et al. A role for differential variable gene pairing in creating T cell receptors specific for unique major histocompatibility ligands. Immunity 2011;35(5):694–704. https://doi.org/10.1016/j.immuni.2011.10.012
[33] Davis MM, Bjorkman PJ. T-cell antigen receptor genes and T-cell recognition. Nature. 1988 Aug 4;334(6181):395-402. doi: 10.1038/334395a0. Errat– : Nat 1988;335(6192):744.
[34] Savir Y, Waysbort N, Antebi YE, et al. Balancing speed and accuracy of polyclonal T cell activation: a role for extracellular feedback. BMC Syst Biol 2012;6:111. https://doi.org/10.1186/1752-0509-6-111
[35] Mayer A, Zhang Y, Perelson AS, Wingreen NS. Regulation of T cell expansion by antigen presentation dynamics. Proc Natl Acad Sci Usa 2019;116(13):5914–9. https://doi.org/10.1073/pnas.1812800116
[36] Farber DL. Biochemical signaling pathways for memory T cell recall. Semin Immunol 2009;21(2):84–91. https://doi.org/10.1016/j.smim.2009.02.003
[37] Kavazović I, Polić B, Wensveen FM. Cheating the hunger games; mechanisms controlling clonal diversity of CD8 effector and memory populations. Front Immunol 2018;9:2831. https://doi.org/10.3389/fimmu.2018.02831
[38] Sasaki K, Moussawy MA, Abou-Daya KI, et al. Activated-memory T cells influence naïve T cell fate: a noncytotoxic function of human CD8 T cells. Commun Biol 2022;5:634. https://doi.org/10.1038/s42003-022-03596-2
[39] Curtsinger JM, Lins DC, Mescher MF. CD8+ memory T cells (CD44high, Ly-6C+) are more sensitive than naive cells to (CD44low, Ly-6C-) to TCR/CD8 signaling in response to antigen. J Immunol 1998;160(7):3236–43.
[40] Kosmrlj A, Jha AK, Huseby ES, Kardar M, Chakraborty AK. How the thymus designs antigen-specific and self-tolerant T cell receptor sequences. Proc Natl Acad Sci USA 2008;105(43):16671–6. https://doi.org/10.1073/pnas.0808081105
[41] Stadinski B, Shekhar K, Gómez-Touriño I, et al. Hydrophobic CDR3 residues promote the development of self-reactive T cells. Nat Immunol 2016;17:946–55. https://doi.org/10.1038/ni.3491
[42] Logunova NN, Kriukova VV, Shelyakin PV, Egorov ES, Pereverzeva A, Bozhanova NG, et al. MHC-II alleles shape the CDR3 repertoires of conventional and regulatory naïve CD4$^+$ T cells. Proc Natl Acad Sci USA 2020;117(24):13659–69. https://doi.org/10.1073/pnas.2003170117
[43] Kosmrlj A, Read EL, Qi Y, Allen TM, Altfeld M, Deeks SG, et al. Effects of thymic selection of the T-cell repertoire on HLA class I-associated control of HIV infection. Nature 2010;465(7296):350–4. https://doi.org/10.1038/nature08997
[44] Price DA, Asher TE, Wilson NA, Nason MC, Brenchley JM, Metzler IS, et al. Public clonotype usage identifies protective Gag-specific CD8+ T cell responses in SIV infection. J Exp Med 2009;206(4):923–36. https://doi.org/10.1084/jem.20081127
[45] von Essen MR, Kongsbak M, Geisler C. Mechanisms behind functional avidity maturation in T cells. Clin Dev Immunol 2012;2012:163453. https://doi.org/10.1155/2012/163453
[46] Campillo-Davo D, Flumens D, Lion E. The quest for the best: how TCR affinity, avidity, and functional avidity affect TCR-engineered T-cell antitumor responses. Cells 2020;9(7):1720. https://doi.org/10.3390/cells9071720
[47] Wang GC, Dash P, McCullers JA, Doherty PC, Thomas PG. T cell receptor ab diversity inversely correlates with pathogen-specific antibody levels in human cytomegalovirus infection. Sci Transl Med 2012;4:128ra42.
[48] Ochi T, Nakatsugawa M, Chamoto K, Tanaka S, Yamashita Y, Guo T, et al. Optimization of T-cell reactivity by exploiting TCR chain centricity for the purpose of safe and effective antitumor TCR gene therapy. Cancer Immunol Res 2015;3(9):1070–81. https://doi.org/10.1158/2326-6066.CIR-14-0222
[49] Nakatsugawa M, Yamashita Y, Ochi T, Tanaka S, Chamoto K, Guo T, et al. Specific roles of each TCR hemichain in generating functional chain-centric TCR. J Immunol 2015;194(7):3487–500. https://doi.org/10.4049/jimmunol.1401717
[50] Kalinina AA, Nesterenko LN, Bruter AV, Balunets DV, Chudakov DM, Izraelson M, et al. Adoptive immunotherapy based on chain-centric TCRs in treatment of infectious diseases. iScience 2020;23:101854–79. https://doi.org/10.1016/j.isci.2020.101854
[51] Zamkova M, Kalinina A, Silaeva Y, Persiyantseva N, Bruter A, Deikin A, et al. Dominant role of the a-chain in rejection of tumor cells bearing a specific alloantigen in TCRa transgenic mice and in in vitro experiments. Oncotarget 2019;10:4808–21. https://doi.org/10.18632/oncotarget.27093
[52] Kalinina A, Bruter A, Persiyantseva N, Silaeva Y, Zamkova M, Khromykh L, et al. Safety evaluation of the mouse TCRα - transduced T cell product in preclinical models in vivo and in vitro. Biomed Pharm 2022;145:112480. https://doi.org/10.1016/j.biopha.2021.112480